Tumor methylation markers and clinical outcome of primary oral squamous cell carcinomas

Clausen, Martijn

DOI:
10.33612/diss.113437849

Chapter 3

Identification and validation of WISP1 as an epigenetic regulator of metastasis in oral squamous cell carcinoma

M.J.A.M. Clausen[1,2], L.J. Melchers[1,2,] M.F. Mastik[1], L. Slagter-Menkema[1, 3], H.J.M. Groen[4], B.F.A.M. van der Laan[3], W. van Criekinge[6], T. de Meyer[6], S. Denil[6], G.B. A. Wisman[5], J.L.N. Roodenburg[2], E. Schuuring[1]

[1] Departments of Pathology, University of Groningen, University Medical Center Groningen, Groningen, the Netherlands.
[2] Departments of Oral and Maxillofacial Surgery, University of Groningen, University Medical Center Groningen, Groningen, the Netherlands.
[3] Departments of Otorhinolaryngology/Head & Neck Surgery, University of Groningen, University Medical Center Groningen, Groningen, the Netherlands.
[4] Departments of Pulmonology, University of Groningen, University Medical Center Groningen, Groningen, the Netherlands.
[5] Departments of Gynecologic Oncology, University of Groningen, University Medical Center Groningen, Groningen, the Netherlands.
[6]Department of Data Analysis and Mathematical Modelling, Ghent University, Ghent, Belgium

Published: Genes Chromosomes Cancer. 2016 Jan;55(1):45-59. doi: 10.1002/gcc.22310.

ABSTRACT

Lymph node (LN) metastasis is the most important prognostic factor in oral squamous cell carcinoma (OSCC) patients. However, in approximately one third of OSCC patients' nodal metastases remain undetected, and thus are not adequately treated. Therefore, clinical assessment of LN metastasis needs to be improved. The purpose of this study is to identify DNA methylation biomarkers to predict LN metastases in OSCC.

Method:

Genome wide methylation assessment was performed on six OSCC with (N+) and six without LN metastases (N0). Differentially methylated sequences were selected based on the likelihood of differential methylation and validated using an independent OSCC cohort as well as OSCC from The Cancer Genome Atlas (TCGA). Expression of WISP1 using immunohistochemistry was analyzed on a large OSCC cohort (n=204).

Results:

MethylCap-Seq analysis revealed 268 differentially methylated markers. WISP1 was the highest-ranking annotated gene that showed hypomethylation in the N+ group. Bisulfite pyrosequencing confirmed significant hypomethylation within the WISP1 promoter region in N+ OSCC ($p = 0.03$) and showed an association between WISP1 hypomethylation and high WISP1 expression ($p = 0.01$). Both these results were confirmed using 148 OSCC retrieved from the TCGA database. In a large OSCC cohort high WISP1 expression was associated with LN metastasis ($p = 0.05$), disease-specific survival ($p = 0.022$) and regional disease-free survival ($p = 0.027$).

Conclusion:

These data suggest that WISP1 expression is regulated by DNA methylation and that WISP1 hypomethylation contributes to LN metastasis in OSCC. WISP1 protein and WISP1 DNA methylation levels are potential biomarkers for identifying OSCC patients who require neck dissection treatment.

INTRODUCTION

Oral Squamous Cell Carcinoma (OSCC) is the most common subtype of Head and Neck Squamous Cell Carcinomas (HNSCC). These OSCC are characterized by a low 5-year survival of 48% [1]. OSCC tends to metastasize to the lymph nodes (LN) before distant metastasis occurs. The presence of these LN metastases has a major impact on OSCC patient survival and is therefore the most important prognostic factor [221]–[223]. Hence, status of the lymph node (N-status) significantly contributes to the selection of current treatment options. Patients with clinically positive N-status (cN+) are generally treated by a neck dissection, which causes mutilation and severe co-morbidity. Clinically negative N-status (cN0) patients are subjected to either an elective neck dissection or a "watchful waiting policy". Therefore, accurate assessment for the presence of lymph node metastases is essential for appropriate treatment management. However, clinical N-status assessment by palpation is inaccurate with a rate of occult LN metastases of 17-30% [49], [224]. In addition, current imaging modalities to determine clinical N-status in palpation-negative necks have a sensitivity of only 60-70% [18], [170]. Thus, to avoid under- and overtreatment, novel prognostic tumor markers are needed.

DNA methylation has been established as important regulator of tumorigenesis and affects cancer progression, metastatic potential, therapy response and patient survival (reviewed in [225]). Through the physical alteration of the cytosine nucleotide by methylation, changes occur in the DNA structure influencing gene transcription (reviewed in [94]). Patterns in genome-wide DNA methylation are cell specific, heritable and influence phenotypes allowing for the prediction of biological behavior of cancer cells (reviewed in [97], [226]). In the clinic, DNA methylation of genes, such as MGMT [227], can be used to predict treatment response, clinical outcome and clinical tumor characteristics including LN metastasis [228]. For instance, LN metastasis in HNSCC has been shown to be associated with methylation of TWIST1 [229], IGF2 [230], CDKN2A, MGMT, MLH1 and DAPK [231]. However, no improvement in the clinical assessment of N-status in OSCC has been made so far with these markers.

To identify new differentially methylated genes and pathways, various global methylation screening approaches have been reported including Infinium BeadArrays and WGBS (reviewed in [131], [136]). More recently, MethylCap-Seq was reported as an innovative new high-resolution technology to uncover DNA-methylation [232] in a genome-wide manner (reviewed in [136]). The approach is based on the identification of DNA CpG methylation by capturing DNA fragments with the Methyl Binding Domain of proteins as MeCP2 and MBD2 followed by next-generation nucleotide sequence analysis on e.g. an Illumina GA platform. Recently, we applied this assay to assess global methylation patterns in OSCC patients with histologically confirmed metastasis positive N-status (pN+) and compared those to OSCC with histopathologically confirmed negative N-status (pN0) or cN0 status for at least two year (Clausen et al., manuscript in preparation). In total 268 regions of differential methylation called Methylation Cores (MC) were identified as potential predictors of N-status. The majority of MC were hypermethylated in pN+ OSCC and only few hypomethylated loci were identified (17%) (Clausen et al., manuscript in preparation). In the present paper, we report on the detailed characterization of the WISP1 (WNT1-inducible-signaling pathway protein 1) gene that we identified as the most significantly hypomethylated annotated gene in

pN+ OSCC and which might act as a new potential diagnostic marker to identify OSCC with LN metastasis. Expression of WISP1 in malignancies other than OSCC was previously reported, but here we describe that high WISP1 expression in a large cohort of primary OSCC is a predictor for the presence of lymph node metastasis. In addition, to our knowledge we describe for the first time that WISP1 promoter methylation levels are associated with pN+ status and WISP1 expression levels in OSCC.

MATERIALS AND METHODS

Patient selection

All patients and carcinomas used in this study were selected from a large cohort described previously [18], [49]. Briefly, Netherlands Cancer Registry records and patient characteristics were collected of all patients with OSCC treated in the University Medical Center Groningen (UMCG) between 1997 and 2008. All patients had no history of prior treatment for HNSCC or other tumors. The histopathological diagnoses were revised for all cases by an experienced head and neck pathologist using the original haematoxylin and eosin (HE)-slides of the formalin-fixed, paraffin embedded (FFPE) tissue blocks. Patient and tumor characteristics are presented in Table 3.1. All cases were treated by primary tumor resection and a neck dissection. To ensure that pN0 cases do not contain occult LN metastases, we included only tumors with histologically confirmed pN0 status and cN0 status after > 2 years of follow-up. For the immunohistochemical study, we used 227 OSCC assembled in triplicate on in total five tissue-microarrays (TMA) as described previously [49]. Each TMA contains seven different normal tissues used as controls as well as for TMA orientation and recognition. All OSCC used in this study were tested for active high-risk HPV16 according to the algorithm of Smeets and colleagues [233]. In total five patients tested positive [49]. For the validation of clinical outcome, only patients with HPV-negative OSCC were included. For the MethylCap-Seq study, six pN+ cases and six pN0 cases were selected from the total cohort. Cases were matched for age and primary tumor site. Leukocytes were acquired from healthy women and served as controls for endogenous methylation and methylation background estimation of tumor samples [234], [235]. All patient tissues were coded. This study was performed according to the Code of Conduct for proper secondary use of human tissue in the Netherlands (www.federa.org), as well as to the relevant institutional and national guidelines.

Table 3.1. Patients characteristics of the UMCG and TCGA patient cohorts

N (%)	UMCG	TCGA
Total tumours	204 (100)	147 (100)
Total patients	204 (100)	147 (100)
Gender		
Male	127 (62)	100 (68)
Female	77 (38)	47 (32)
Age at diagnosis (yrs)		
Median	63	61
Range	35-94	19-87
Site		
Tongue	58 (28)	80 (54)
Floor of mouth	69 (34)	26 (18)
Cheek mucosa	7 (3)	0 (0)
Gum	24 (12)	41 (28)
Retromolar area	14 (7)	0 (0)
Oropharynx	27 (13)	0 (0)
Other	5 (3)	0 (0)
cN status		
0	125 (61)	73 (50)
+	79 (39)	73 (50)
pT status		
01-02	129 (63)	17 (12)
03-04	75 (37)	42 (28)
pN status		
pN0	104 (51)	61 (42)
pN+	100 (49)	86 (58)
Extranodal spread (only pN+)		
No	64 (57)	40 (47)
Yes	48 (43)	26 (30)
Perineural invasion		
No	133 (72)	51 (35)
Yes	51 (28)	69 (47)
Lymphovascular invasion		
No	144 (85)	83 (57)
Yes	26 (15)	31 (21)
Histological differentiation		
Well	50 (23)	18 (12)
Moderate	130 (61)	102 (69)
Poor	34 (16)	27 (18)
HPV16 status		
Negative	191 (97)	28 (97)
Positive	5 (3)	1 (3)
Infiltration depth (mm) (n = 181)		
Median	9.3	Not available
Range	0.07 – 40	Not available

DNA isolation

DNA isolation was performed as reported previously [236]. Briefly, two 10 µm thick FFPE sections were deparaffinized in xylene and incubated overnight in 300 µl 1% SDS-proteinase K at 60ºC. Subsequently, DNA was extracted using phenol-chloroform extraction and ethanol precipitation. DNA pellets were washed with 70% ethanol, dissolved in 50 µl TE^{-4} (10 mM Tris/HCL; 0.1 mM EDTA, pH 8.0) and stored at 4ºC. Genomic DNA was amplified in a multiplex PCR according to the BIOMED-2 protocol to check the DNA's structural integrity [196]. Only cases with products ≥200 bp were included for further analyses. For the MethylCap-Seq samples, DNA was extracted from snap frozen material. Then DNA quantity was measured using Quant-iT™ PicoGreen® dsDNA Assay Kit according to manufacturer's protocol (Invitrogen, Carlsbad, CA, USA). For OSCC in the validation cohort, DNA concentrations and 260/280 ratios were measured using the Nanodrop ND-1000 Spectrophotometer (Thermo Scientific, Waltham, MA, USA). A 260/280 ratio of >1.8 was required for all samples. A 3 µm thick section was HE-stained to check for tumor load. Only cases with at least 60% tumor cells were included in this study.

MethylCap-Seq analysis

MethylCap-Seq was performed to assess genome-wide methylation of 12 OSCC and two pools of leukocytes by capturing fragmented DNA with the Methyl Binding Domain protein MeCP2 followed by paired-end next generation sequencing on the Illumina GA II as reported previously [151], [232]. In summary, 500 ng DNA was fragmented using Covaris S2 (Covaris, Woburn, MA, USA) and methylated DNA fragments were captured with the MethylCap kit (Diagenode, Belgium) according to the manufacturer's protocol. Subsequently, the captured fragments were paired-end-sequenced using the Illumina Genome Analyzer II (Illumina, San Diego, CA, USA). The sequenced paired-ends were mapped to the human reference genome (NCBI build 37.3) using BOWTIE software [237]. Reads were included when the paired-end fragments were mapped to a unique locus and the distance between paired ends after mapping was within 400 bp. Exactly overlapping reads were discarded because these reads are most likely amplifications of the same captured DNA fragment. Mapped reads were summarized using the "Map of the Human Methylome", an in house developed overview of possibly methylated regions, called "Methylation Cores" [168], [382].

All Methylation Cores (MCs) located 2000 bp upstream to 500 bp downstream of the Transcription Start Site (TSS) or in the first exon of an Ensemble (v65) gene were statistically compared using R [238] with R-package Bayseq [239]. MC were ranked according the likelihood of differential methylation and we also calculated an approximate false discovery rate (FDR). The 5000 MC with the lowest FDR were used for further analysis. For all annotated MCs p-values were calculated using the two-sided independent student-t test. Subsequently, the following criteria were applied for further MCs selection: significant p-value ($p < 0.05$); the lowest read count in the relatively hypermethylated group is equal or higher than the highest read count in the relatively hypomethylated group of the pN0 and pN+ OSCC.

Verification and validation of MethylCap-sequencing data of WISP1 by bisulfite pyrosequence analysis.

Methylation levels within the WISP1 gene promoter were determined using bisulfite pyrosequence analysis. Sodium bisulfite treatment of isolated genomic DNA (1 µg/sample) was performed according to the recommendations of the EZ DNA methylation kit (Zymo Research, Corp, Irvine, CA). The efficiency of the cytosine to uracil conversion by bisulfite treatment of each DNA sample was checked by Methylation Specific PCR (MSP) for beta-actin and DAPK as reported previously [139]. All primer sequences and PCR conditions are described in Table 3.2. Pyrosequencing primers for WISP1 (Table 3.2) were designed using Pyromark Assay design version 2.0.1.15 (Qiagen, Hilden, Germany). Bisulfite treated DNA was amplified using the Pyromark PCR kit according to the company's protocol (Qiagen). Each reaction was performed with 12.5 µl PCR master mix 2x, 200 nmol of the forward, 20 nmol of the reverse primer and 180 nmol of a universal biotinylated primer. The reverse primer contained a universal 23 bp DNA tag 5'-GACGGGACACCGCTGATCGTTTA-3' that is recognized by a biotinylated primer as described [140] The PCR was performed as following: 15 min 95°C, 50 cycles of (30 sec 94°C, 30 sec 56°C, 30 sec 72°C), 10 min 72°C. Purification of the PCR product was performed using the Q24 Vacuum Workstation (Qiagen) according to the manufacturer's protocol. The biotinylated PCR products were captured using 1 µl Streptavidin-coated Sepharose High Performace beads (GE Healthcare, Little Chalfont, UK). The immobilized products were washed with 70% alcohol, denatured with PyroMark Denaturation Solution (Qiagen) and washed with PyroMark Wash Buffer (Qiagen). The purified PCR product was then added to 25 µl PyroMark Annealing Buffer (Qiagen) containing 0.3 µM Sequening Primer specific for the WISP1 amplicon. Finally, pyrosequencing was performed using the Pyromark Q24 (Qiagen). Methylation percentages of all measured CpGs were analyzed using the provided Pyromark Q24 software version 2.0.6 (Qiagen). Average methylation of all measured CpG's as well as all individual CpG's were compared between groups. Pyrosequencing measurements considered failed by the Pyromark software were excluded. Incomplete bisulfite conversion threshold was 5%.

Leukocyte DNA from healthy volunteers was used as control for normal/endogeneous methylation levels, in vitro methylated (by SssI enzyme) leukocyte DNA as a positive control for hypermethylation and Whole Genome Amplified (WGA) leukocyte DNA using the illustra Ready-To-Go GenomiPhi HY DNA Amplification Kit (GE Healthcare) as a control for unmethylated DNA. All three controls were included in each bisulfite pyrosequencing run to check for differences between runs.

Immunohistochemistry

Immunohistochemical staining was performed as described previously [49]. Briefly, 3-µm thick sections of FFPE tumor tissue were deparaffinized and rehydrated. Antigen retrieval was performed by citrate buffer in a microwave oven for 15 min at 400 W as previously reported [240]. Endogenous peroxidase was blocked in a 0.3% H_2O_2 solution for 30 min at room temperature (RT). Slides were incubated overnight at 4°C with rabbit polyclonal antibody to human WISP1 (H-55: sc-25441) (Santa Cruz, CA, USA) diluted 1:50 in PBS [240] with 1% Bovine Serum Albumin. Subsequently, the sections were incubated with Envision+ (Dako, Glostrup, Denmark) horseradish peroxidise for 30 min at RT, developed with 3,3–diaminobenzidine

solution (Dako) containing 0.03% H_2O_2 and counterstained with haematoxylin for 2 min. Fallopian tube was used as a positive control for WISP1 expression and pancreas, gallbladder and colon tissue were used as negative controls [241].

Staining intensity was semi-quantitatively scored as reported [240]. The percentage of tumor cells stained and the intensity of staining (0, no staining; 1, weak; 2, moderate; 3, strong). Each staining was scored by two observers independently. Discordant results were discussed until consensus was reached. ROC curve analysis was performed to determine the optimal cut-off between pN0 and pN+ OSCC. Cases with strong staining (3) in > 7.5 % of the tumor cells were considered to have high WISP1 expression.

Table 3.2. Primer Sequences and optimized PCR conditions

Primer	Sequence 5'-3'	Tannealing (°C)
ACTB MSP forward	TAGGGAGTATATAGGTTGGGGAAGTT	57
ACTB MSP reverse	AACACACAATAACAAACACAAATTCAC	57
DAPK1 MSP meth forward	GGATAGTCGGATCGAGTTAACGTC	60
DAPK1 MSP meth reverse	CCCTCCCAAACGCCGA	60
DAPK1 MSP unmeth forward	GGAGGATAGTTGGATTGAGTTAATGTT	60
DAPK1 MSP unmeth reverse	CCCTCCCAAACACCAACC	60
WISP1 pyroseq forward	TTAGTGGTAGTAGTGTAATAAGGGTATAG	54
WISP1 pyroseq reverse	GACGGGACACCGCTGATCGTTTAACTCAAATTACAACATCACCTTCATAAC	54
WISP1 pyroseq sequencing	GTGGGGATAGTTTTAGTATT	54

TCGA data analysis

All cases (n = 148) from The Cancer Genome Atlas (TCGA) database (the TCGA Research Network 2014) were selected with the following criteria; tumor located in either "Floor of Mouth", "Oral Cavity" or "Oral Tongue"; available pN-status and available Level 3 Methylation (Illumina Infinium 450k) data. Additional annotation for the Infinium 450k probe was acquired from the Gene Expression Omnibus (GEO) accession number GSE42409 including distance to TSS, associated CpG island and position [242]. All 450k probes associated with the WISP1 TSS were extracted for further analysis (n = 14). Subsequently, beta-values were quantile normalized by using R (version 3.0.3) to apply the normalizeBetweenArrays function from the R package preprocessCore from Bioconductor [243]. With R and the Lumi package the normalized WISP1 450k probe beta values were converted to M-values using the beta2m function and statistically compared between the pN0 and pN+ OSCC using the eBayes function of the Limma package [244].

Statistical Analysis

Statistical analysis was performed using SPSS version 22.0.1 software package. Associations between WISP1 expression and clinico-pathological characteristics were tested using the χ^2 test. The WISP1 IHC cut-off was optimized using a ROC-curve analysis. Survival was defined as the number of days between the first treatment and disease-specific death (DSS) or disease recurrence (DFS) and analyzed by Kaplan-Meier curves and log rank test. All tests were performed two-tailed and a p-value ≤ 0.05 was considered

statistically significant.

RESULTS

Identification of WISP1 as the most significantly hypomethylated gene in pN+ OSCC.

To assess the genome-wide methylation status of metastatic and non-metastatic OSCC, MethylCap-Seq was performed on six pN0 and six pN+ OSCC primary tumors. On average 10.2 million methylated DNA fragments were captured, sequenced and mapped to the human genome for each of these 12 OSCC DNA samples. The R package BaySeq was used to identify and rank all MC that were differentially methylated between pN0 and pN+ OSCC and located -2000 to 500 bp from a TSS or in the first exon of an Ensemble gene. Using the highest ranking 5000 MC with the lowest FDR, 1609 MC tested significantly different using a two-sided independent student-t test ($p \leq 0.05$). From these 1609 MC, 355 MC were selected for which the lowest read count in the relatively hypermethylated group was higher or equal to the highest read count in the relatively hypomethylated group. Finally, for 268 MC there was an annotated function in the UniProtKB/Swiss-Prot database (supplemental Table 3.1).

The majority of the MC were hypermethylated in pN+ OSCC (84%, 226/268), only 42 of the 268 (16%) selected MC were hypomethylated in pN+ OSCC (supplemental Table 3.1). Table 3.3 shows that of the 15 highest ranking differentially methylated MC, 13 showed higher levels of methylation in the pN+ group, whereas SLC7A10 and WISP1 were higher in the pN0 OSCC. Of these two genes, WISP1 was the highest ranking hypomethylated annotated gene in pN+ in comparison to both pN0 OSCC as well as normal DNA (Table 3.3). The annotated WISP1 MC was located between position 134,202,288 and 134,202,631 on chromosome 8 (GRCh37/hg19), 681 to 1025 bp upstream of the WISP1 TSS [245] (Figure 3.1). According to the GSE42409 "Additional Annotation Information" of the Infinium 450k probes [242], this region contains a CpG island (chr8: 134,202,271 – 134,202,560 bp) (Figure 3.1) [246].

Verification of the association between WISP1 promoter methylation and lymph node status

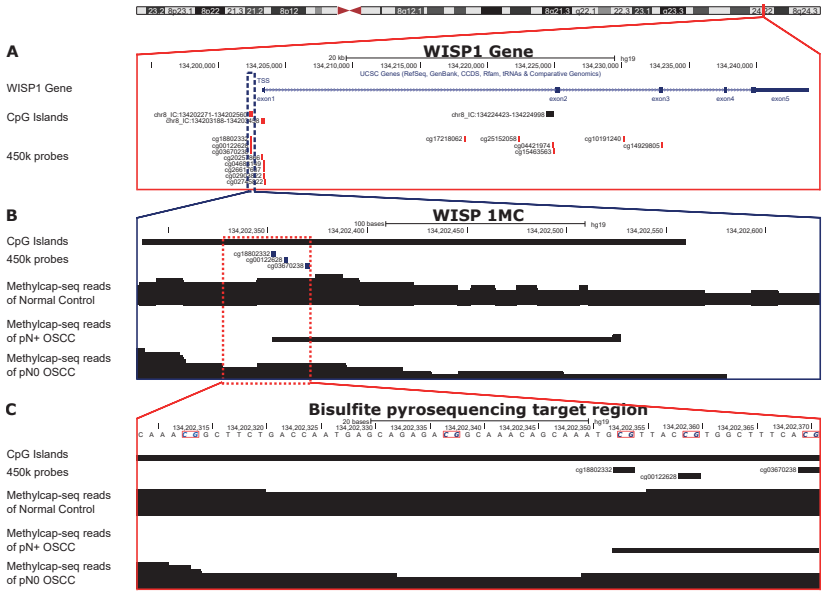

Figure 3.1. The WISP1 differentially methylated region annotated by MethylCap-Seq and the location of the bisulfite pyrosequenced CpGs. A) Schematic representation of the genomic region around the WISP1 gene (chr8:134,201,000 - 134,246,000) as extracted from the UCSC browser (GRCh37/hg19). The Transcription Start Site (TSS) is located at position 134,203,282. B) The WISP1 MC located 134,202,288 - 134,202,631, which is 681 to 1025 bp upstream of the WISP1 TSS, as retrieved from the Map of the Human Methylome [168], [382], the reads retrieved by MethylCap-seq analysis comparing 6 pN+ and 6 pN0 OSCC in this region, the known Infinium 450k probes and CpG Island location as retrieved from the GSE42409 database. C) The genomic region within the WISP1 MC as sequenced by bisulfite pyrosequencing, the reads retrieved by MethylCap-seq analysis comparing 6 pN+ and 6 pN0 OSCC in this region, the known Infinium 450k probes and CpG Island locations as retrieved from the GSE42409 database.

in OSCC

To validate whether the levels of DNA methylation of the selected WISP1 MC is associated with the lymph node status of OSCC, a bisulfite pyrosequencing assay was designed to quantify the methylation of five CpG sites in this WISP1 MC (Figure 3.1). Methylation levels were quantified on an independent validation cohort of 19 OSCC (Figure 3.2). Average (± SEM) methylation levels of all five CpG sites in the 10 pN0 (64 ± 3) and nine pN+ cases (49 ± 6) were both significantly lower than in leukocyte samples (86 ± 1) ($p < 0.01$). Moreover, the average methylation levels of the five CpG sites in pN+ cases were significantly lower than in the pN0 OSCC cases ($p = 0.02$) (Figure 3.2). When we compared the average methylation levels of each CpG site separately, the third CpG of the five pyrosequenced WISP1 MC CpGs showed the most significant difference between pN+ and pN0 ($p < 0.05$) (Figure 3.3 A). In summary, bisulfite pyrosequencing of the WISP1 promoter region in an independent cohort of 19 OSCC confirmed the lower methylation levels in pN+ OSCC as detected from the MethylCap-Seq marker discovery analysis.

Table 3.3. The fifteen highest annotated genes after statistical analysis of the enriched and sequenced reads of MethylCap-Seq.

Rank by False Discovery Rate	Gene name	Average distance to TSS (bp)	MC size (bp)	Average readcount pN0 OSCC	Average readcount pN+ OSCC	Hypermethylated in	False Discovery Rate	P-value student-test
1	ARHGEF4	0	327	1	5	pN+	0.26	0
2	U6	208	404	3	13	pN+	0.34	0.04
3	WISP1	-853	343	6	3	pN0	0.41	0
4	EMX2	-955	194	1	5	pN+	0.43	0
5	KCNIP1	0	298	1	5	pN+	0.44	0.02
6	SOBP	0	384	3	10	pN+	0.48	0.01
7	snoU13	70	286	2	6	pN+	0.48	0
8	GPD2	507	108	0	3	pN+	0.5	0
9	EDNRB	0	212	2	7	pN+	0.56	0.01
10	RAB13	-2092	270	3	8	pN+	0.57	0
11	SLC7A10	0	211	6	3	pN0	0.57	0
12	TAPT1	-2065	444	2	6	pN+	0.6	0
13	C1orf212	-1133	426	3	9	pN+	0.61	0
14	AL078621.5	-341	88	0	3	pN+	0.61	0
15	TMEM75	-591	138	1	4	pN+	0.63	0

All MC were ranked according to False Discovery rate (see supplemental table 3.1). After this ranking for each annotated gene the statistical difference between pN0 and pN+ were calculated by two-sided student t-test. Subsequently all MC were selected for which: the lowest read count in the relatively hypermethylated group is equal or higher than the highest read count in the relatively hypomethylated group of the pN0 and pN+ OSCC and there was an annotated description in the UniProtKB/Swiss-Prot database.

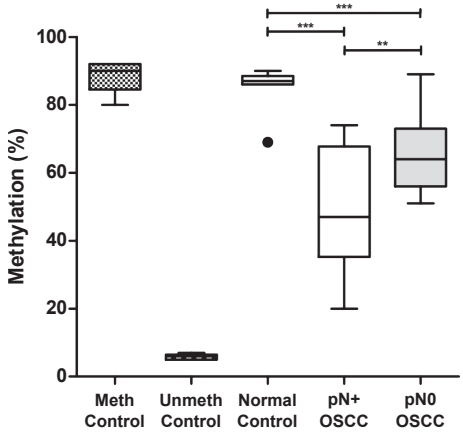

Figure 3.2. Methylation levels of the WISP1 MC are lower in pN+ OSCC compared to pN0 OSCC. The average methylation of the 5 WISP1 CpG sites were determined in 10 pN+ and 9 pN0 OSCC by bisulfite pyrosequence analysis. DNA from leukocytes from healthy controls was used as control for normal/endogenous methylation levels (Normal Control), in vitro methylated leukocyte DNA as a positive control for DNA methylation (Meth Control) and Whole Genome Amplified leukocyte DNA as an unmethylated DNA control (Unmeth Control). (* = p-value ≤ 0.1, ** = p-value ≤ 0.05, *** = p-value ≤ 0.01).

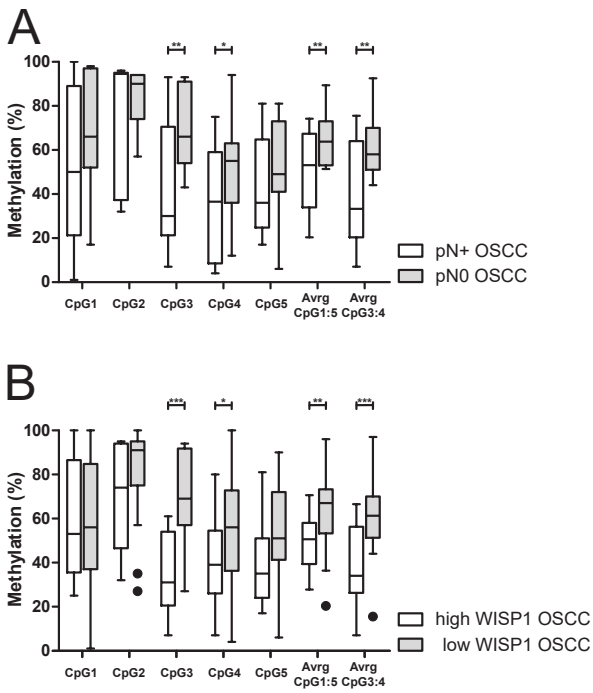

Figure 3.3. Methylation levels of the WISP1 promoter differ between pN0 and pN+ OSCC as well as between low and high WISP expressing OSCC. A) The methylation status of 5 CpG sites in the WISP1 MC was determined in 10 pN+ and 9 pN0 OSCC by bisulfite pyrosequencing. The methylation percentages of each individual CpG sites were compared between groups in addition to the average methylation percentage of all 5 CpG sites and the average of CpG sites 3 and 4. B) The methylation status of the same 5 CpG sites in the WISP1 MC was determined in 8 high WISP1 expressing OSCC and 16 low WISP1 expressing cases. The methylation percentages of each individual CpG sites were compared between groups in addition to the average methylation percentage of all 5 CpG sites and the average of CpG sites 3 and 4. (* = p-value ≤ 0.1, ** = p-value ≤ 0.05, *** = p-value ≤ 0.01).

To confirm the association between methylation of the WISP1 promoter region and lymph node status in OSCC, we used OSCC present in the TCGA database as independent validation cohort. For this purpose, 148 patients were selected with OSCC for which both the pN-status as well as well methylation data were available. In total 14 probes were identified that are associated with the WISP1 TSS, located -6996 to 7689 bp from the WISP1 TSS (Figure 3.1). 3 of these probes overlapped with the WISP1 MC and the CpGs in the WISP1 MC pyrosequenced region (Figure 3.1). All 14 probes were found to be significantly differentially methylated between pN0 (n = 61) and pN+ (n = 87) (supplemental table 3.2). Moreover, all three probes (cg18802332, cg00122628, cg03670238) overlapping with the bisulfite pyrosequencing assay were hypomethylated in the pN+ OSCC compared to the pN0 OSCC (supplemental table 3.2), in agreement with the bisulfite pyrosequence data. The analysis of the TCGA data confirms that hypomethylation of the WISP1 region is characteristic for pN+ OSCC.

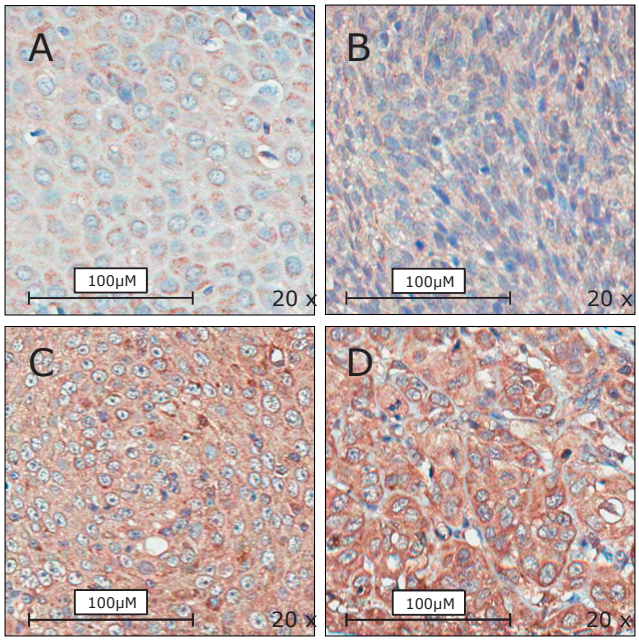

Figure 3.4. Representative examples of the different WISP1 intensity in 4 OSCC using immunohistochemistry. Tissues were scored for both immunoreactivity intensity ((A) no staining, (B) weak, (C) moderate; (D) strong staining and percentage of positive neoplastic cells. Cases with strong staining in >7.5 % of the neoplastic cells were considered as high WISP1 expressers and all other patterns as negative/low.

WISP1 promoter methylation in association with WISP1 expression

To validate whether WISP1 methylation levels are associated with WISP1 expression levels, bisulfite pyrosequencing of the WISP1 promoter region was performed on 21 OSCC cases with very high (score 2-3 in 100% of tumor cells) or low (negative or score 0-1) WISP1 protein expression as determined by immunohistochemistry. Average methylation levels of the five CpG sites were significantly lower ($p < 0.05$) in eight high WISP1 expressing OSCC compared to 16 low WISP1 expressing cases (Figure 3.3 B). Analysis of the separate CpG sites revealed that methylation levels of CpG3 ($p < 0.05$) and CpG3-4 ($p < 0.01$) were significantly lower in high WISP1 expressing OSCC ($p < 0.05$) (Figure 3.3 B).

High WISP1 expression in primary OSCC is a predictor for lymph node metastasis and clinical outcome

To validate whether WISP1 expression is associated with clinical outcome in OSCC, immunohistochemistry was performed on a cohort of 227 pretreatment biopsies of patients with OSCC of which clinic-pathological and follow-up data are available. Because 23 cores were lost during immunostaining or cores did not contain enough tumor cells anymore, WISP1 immunostaining could be assessed on 204 OSCC cases (see examples in Figure 3.4). High WISP1 expression was observed in 49 of 204 OSCC (24%) and found to be significantly associated with pN+ status ($p = 0.05$) (Table 3.4). Expression of WISP1 was also correlated with poor tumor differentiation ($p = 0.041$) but not with any of the other clinico-pathological features (Table 3.4).

Table 3.4. Clinical characteristics of OSCC patients with low or high WISP1 protein levels measured by IHC.

	Low WISP1 OSCC N (%)	High WISP1 OSCC N (%)	P-value
Total tumours	155 (76)	49 (24)	
Total patients	155 (76)	49 (24)	
Gender			
Male	97 (76)	30 (24)	0.864
Female	58 (75)	19 (25)	
Age at diagnosis (yrs)			
Median	63	62	0.199
Range	35-94	36-89	
Site			
Tongue	46 (79)	12 (21)	0.483
Gum	21 (88)	3 (12)	0.16
Retromolar area	11 (79)	3 (21)	0.814
Cheek mucosa	6 (86)	1 (14)	0.54
Floor of mouth	52 (75)	17 (25)	0.883
Oropharynx	15 (56)	12 (44)	0.056
Other	4 (80)	1 (20)	0.831
cN status			
0	99 (79)	26 (21)	0.176
+	56 (71)	23 (29)	
pT status			
01-02	98 (76)	31 (24)	0.996
03-04	57 (61)	37 (39)	
pN status			
0	85 (82)	19 (18)	0.05
+	70 (70)	30 (30)	
Extranodal spread (only pN+)			
No	37 (67)	18 (33)	0.511
Yes	33 (73)	12 (27)	
Perineural invasion			
No	106 (80)	27 (20)	0.188
Yes	36 (71)	15 (29)	
Lymphovascular invasion			
No	115 (80)	29 (20)	0.227
Yes	18 (69)	8 (31)	
Histological differentiation			
Well	41 (87)	6 (13)	0.041
Moderate or Poor	106 (73)	40 (27)	
HPV16 status			
Negative	146 (76)	45 (26)	0.061
Positive	2 (40)	3 (60)	
Infiltration depth (mm) (n = 181)			
Median	7	9	0.114
Range	0.07 - 30	2.10 - 40	
Infiltration depth (mm) (n = 200)			
<4 mm	25 (83)	5 (17)	0.318
>4 mm	113 (75)	38 (25)	

In order to assess the association between WISP1 expression and clinical outcome Kaplan-Meier log-rank analysis was performed on our OSCC cohort. To correct for different survival between HPV-positive and HPV-negative OSCC, only OSCC patients that were tested HPV-negative were included in this analysis. Kaplan-Meier log-rank analysis revealed a significant correlation between high WISP expression and worse disease-specific survival (Figure 3.5A, p = 0.022) as well as worse regional disease-free survival (Figure 3.5B, p = 0.027).

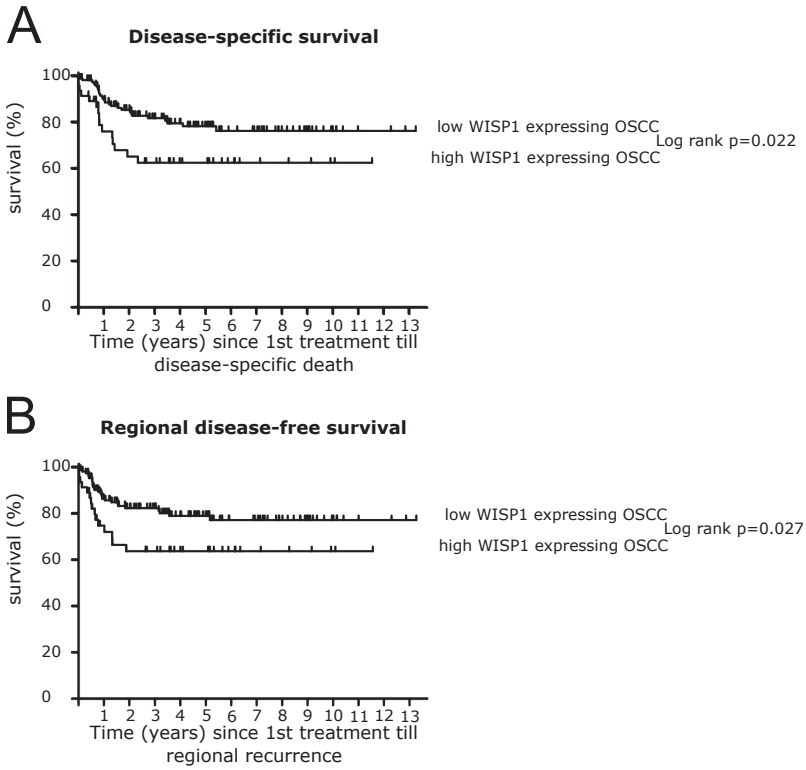

Figure 3.5. Kaplan–Meier curves of (A) Disease-specific survival stratified according to WISP1 expression for all HPV16 negative OSCC; and (B) Regional disease-free survival stratified according to WISP1 expression for all HPV16 negative OSCC. P-values of Log rank analysis.

DISCUSSION

During carcinogenesis the expression of cancer-associated genes is altered by changes in promoter methylation. These changes are thought to be an important event in tumor progression, therapy response, invasion and metastasis [225]. Therefore, the generation of a methylome specific for certain stages of disease in OSCC might be very helpful to gain new insight in OSCC carcinogenesis and to develop new tools for diagnosis and prognosis. Various studies have reported methylation markers in head and neck cancer, but today only few genes have been associated with lymph node status [247]–[249], clinical outcome and treatment response [250], [251]. Moreover, none of these markers showed sufficient predictive value for detecting the presence of lymph node metastases in early OSCC and clinical application [228], [252]. To identify new methylation markers associated with pN-status in OSCC, we performed a genome-wide methylation analysis using MethylCap-Seq as described recently [232]. This analysis revealed that of all differentially methylated markers, the WISP1 gene was the highest annotated hypomethylated gene in the OSCC with lymph node metastases (pN+) when compared to both OSCC without lymph node metastases (pN0) and leukocytes from healthy controls. In the present paper, we report on the identification and characterization of the association between DNA hypomethylation of the WISP1 gene and the presence of lymph node metastases in OSCC. We showed that WISP1 expression was correlated with DNA methylation of its promoter, and that decreased methylation levels were associated with increased WISP1 expression. In addition, using a large OSCC cohort (n = 204) high WISP1 expression was significantly associated with lymph node metastasis ($p = 0.05$) in 204 OSCC as well as with DFS ($p = 0.022$) and DSS ($p = 0.027$) in 191 HPV negative OSCC. Our data suggest that WISP1 is a new prognostic marker to predict OSCC metastasis to the regional lymph nodes.

WISP1 expression was observed before in other cancers [240], [253]–[259]. However, we describe for the first-time decreased DNA methylation levels of WISP1 in primary OSCC of patients with lymph node metastases. WISP1 DNA methylation was found 681 to 1025 bp upstream of the WISP1 TSS in a CpG island [193], [242]. We also showed that decreased WISP1 promoter DNA methylation was associated with high WISP1 expression. These findings suggest that hypomethylation of the WISP1 promoter in pN+ OSCC could be responsible for the up regulation of the WISP1 gene in metastatic OSCC. Using bisulfite pyrosequencing, we confirmed the increased WISP1 DNA methylation levels in OSCC cases with low WISP1 expression, whereas in pN+ OSCC decreased WISP1 DNA methylation levels were associated with a high WISP1 expression. Therefore, our data imply that WISP1 promoter methylation is as a potential new mechanism to regulate WISP1 expression in tumor cells. To confirm WISP1 DNA hypomethylation in pN+ OSCC on a larger independent cohort, we selected 148 OSCC cases present in the TCGA database from which also pN and methylation data were available. All 14 probes in the Infinium 450k platform located in the WISP1 promoter region were significantly differentially methylated between pN0 and pN+ OSCC. In particular, the three probes in the Infinium 450k platform located in the WISP1 MC identified by MethylCap-Seq analysis were also significantly hypomethylated in pN+ OSCC in agreement with our MethylCap-Seq and bisulfite pyrosequencing data.

It is now generally accepted that during cancer progression overall methylation decreases while gene promoter methylation increases especially of tumor suppressor genes [97]. Consequently, hypermethylation is thought to be correlated with tumor progression and metastasis [252]. In contrast to these tumor suppressor genes, we now found that WISP1 was hypomethylated in progressed disease as defined by the presence of lymph node-metastases. WISP1 DNA methylation levels were not only lower compared to pN0 OSCC but also to normal leucocytes suggesting that during progression of disease, WISP1 becomes actively hypomethylated. We also showed that the majority of the highest ranking differentially methylated MC other than WISP1 (see supplemental Table 3.2) were hypermethylated in pN+ OSCC (84%,226/268), whereas hypomethylation in the pN+ group was found only sporadically (16%, 42/268). Also in other studies, demethylation during cancer progression [260] in HNSCC has been reported for few other genes (MAGEB2, CSPG4 and ALK [247], [261], [262]), imprinted genes like Insuline-like growth factor 2 [263], repetitive elements Alu [264] and LINE-1 [265]. In addition, decreased DNA methylation levels associated with worse clinical outcome or response to chemoradiation has been described for a number of genes including TGM2, ASS1, TP73 and RASSF1A (reviewed in [174]). Based on increased DNA methylation levels of promoter sequences of tumor suppressor genes and their association with progressive disease in general[97], demethylating agents like 5-aza-2'-deoxycytidine might be a powerful new treatment strategy and in fact has already been implicated in e.g. acute myeloid leukemia[266]. However, our observations now strongly suggest that clinical treatment strategies using demethylating agents might be harmful for patients with OSCC, since upon treatment WISP1 might be de-methylated and re-expressed resulting in an increased metastatic potential.

WISP1, or WNT1-inducible-signaling pathway protein 1, belongs to the CCN protein family of six homologous, cysteine-rich secreted proteins induced by the Wnt-pathway. All CCN proteins are known to be involved in cancer related processes like cell adhesion, cell migration, proliferation and cell survival [267]. Moreover, WISP1 expression has been connected to the cancer promoting Notch pathway [256] and the Wnt-pathway [259] which are known to be abnormal in HNSCC [268] and is thought to contribute to lymph node metastasis in OSCC [269]. WISP1 has also been reported to influence P53 mediated-apoptosis by activating AKT [270] which is downstream in the ALK pathway [271].Subsequently, WISP1 over expression has been correlated with cancer progression, poor survival and metastasis in breast cancer [258], colorectal cancer [254], rectal cancer [257], esophageal squamous cell carcinoma [240] and NSCLC [253]. Interestingly, other published methylation markers that predict lymph node metastasis in OSCC are ALK, which is linked with WISP1 activity through AKT [247] and two genes which interact with WISP1 through the Wnt-pathway: RUNX3 and WIF1 [249]. In summary, our data suggest that WISP1 expression is regulated by DNA methylation and that WISP1 de-methylation contributes to lymph node metastasis in patients with OSCC. WISP1 DNA methylation and expression might contribute to a better selection of patients that might benefit from more optimal therapy. This will result in better patient survival and quality of life for OSCC patients. Therefore, WISP1 DNA methylation levels in primary OSCC could be used in deciding whether to treat patients shown to be cN0 by imaging with neck dissection.

Supplemental table 3.1. All 268 selected genes after statistical analysis of the enriched and sequenced reads of MethylCap-Seq.

All MC were ranked according to False Discovery rate. After this ranking for each annotated gene the statistical difference between pN0 and pN+ were calculated by two-sided student t-test. Subsequently all MC were selected for which: the lowest read count in the relatively hypermethylated group is equal or higher than the highest read count in the relatively hypomethylated group of the pN0 and pN+ OSCC and there was an annotated description in the UniProtKB/Swiss-Prot database.

Rank by False Discovery Rate	Gene name	Average distance to TSS (bp)	MC size (bp)	Average readcount pN0 OSCC	Average readcount pN+ OSCC	Hypermethylated in	False Discovery Rate	P-value student-test
1	ARHGEF4	0	327	1	5.3	pN+	0.26	0
2	U6	208	404	2.7	13.2	pN+	0.34	0.04
3	WISP1	-853	343	5.8	2.5	pN0	0.41	0
4	EMX2	-955	194	1	4.8	pN+	0.43	0
5	KCNIP1	0	298	0.5	4.7	pN+	0.44	0.02
6	SOBP	0	384	3	9.7	pN+	0.48	0.01
7	snoU13	70	286	1.5	6.2	pN+	0.48	0
8	GPD2	507	108	0	2.5	pN+	0.5	0
9	EDNRB	0	212	1.8	6.5	pN+	0.56	0.01
10	RAB13	-2092	270	2.5	7.8	pN+	0.57	0
11	SLC7A10	0	211	6.2	3	pN0	0.57	0
12	TAPT1	-2065	444	1.7	5.8	pN+	0.6	0
13	C1orf212	-1133	426	3.3	9.3	pN+	0.61	0
14	AL078621.5	-341	88	0.2	2.7	pN+	0.62	0
15	TMEM75	-591	138	0.8	4	pN+	0.63	0
16	hsa-mir-516a-2	-579	217	1.7	6	pN+	0.64	0.01
17	APH1A	0	57	2.2	0.3	pN0	0.64	0
18	Y_RNA	611	396	1	4.3	pN+	0.65	0.01
19	SMOC2	455	178	1	4.7	pN+	0.66	0.02
20	HHLA2	-1128	167	1.3	5	pN+	0.67	0.01
21	SGPL1	-1927	130	2	0.2	pN0	0.68	0.01
22	NFE2L1	-1806	86	0	2.2	pN+	0.68	0
23	TMEM117	-763	123	0.2	2.5	pN+	0.7	0
24	OR2B11	-404	188	1.7	5.5	pN+	0.71	0
25	EMR2	-1322	151	1	4.2	pN+	0.71	0.01
26	DLGAP4	-381	391	0.7	3.5	pN+	0.72	0.01
27	AC084125.1	-841	226	2.7	7.5	pN+	0.72	0
28	ACTA1	-756	273	0.7	3.7	pN+	0.73	0.02
29	DYRK1A	-1938	22	0.5	3	pN+	0.73	0
30	PHYHIP	-303	289	2.7	7.5	pN+	0.73	0
31	AAMP	0	539	4.7	11.5	pN+	0.74	0
32	PAX7	169	293	0.7	3.7	pN+	0.75	0.03
33	SEC31B	-684	302	2	6	pN+	0.76	0
34	TOR1A	-1925	127	1.8	0.2	pN0	0.76	0.01
35	EXOSC6	0	202	1.3	4.7	pN+	0.76	0
36	AC010645.1	-1721	296	3.3	8.7	pN+	0.76	0
37	TMEM110	0	169	2.5	7.2	pN+	0.77	0.01
38	DEDD	-1674	232	1.5	4.8	pN+	0.77	0
39	TINAG	0	81	0.5	3.2	pN+	0.78	0.02
40	EPM2AIP1	0	150	3	1.2	pN0	0.78	0.01
41	EGR4	611	636	1	4	pN+	0.79	0.01
42	TRABD	-1948	358	5.5	3	pN0	0.79	0.03
43	PCK1	0	47	1.5	5	pN+	0.79	0.01
44	ZDBF2	97	203	0	2	pN+	0.8	0
45	FAM107B	-370	123	1.3	4.5	pN+	0.81	0.01
46	RHOD	-620	72	0.2	2.2	pN+	0.81	0
47	GRIK5	90	199	1.7	5	pN+	0.81	0
48	LIN7B	-1501	197	0.5	2.8	pN+	0.81	0
49	snoU13	172	127	0.8	3.5	pN+	0.82	0.01
50	RPS6KB1	0	417	3.2	8	pN+	0.82	0
51	Y_RNA	-855	298	1.8	5.3	pN+	0.82	0
52	ASB3	-2017	164	1.7	5	pN+	0.83	0
53	AIM1	0	155	0.7	3.2	pN+	0.83	0.02
54	snoU13	404	293	2.7	7	pN+	0.83	0
55	VPS33A	-1192	233	1.8	5.3	pN+	0.83	0
56	SH3YL1	-274	227	2	5.7	pN+	0.83	0
57	ZDHHC8P	304	331	2	0.5	pN0	0.83	0.01

58	RAP1GAP	-384	536	0.2	2.2	pN+	0.83	0.01
59	DUS3L	-302	297	3.2	7.8	pN+	0.83	0
60	AB019438.11	591	221	0.8	3.3	pN+	0.84	0
61	SRP_euk_arch	-193	46	1	3.7	pN+	0.84	0.01
62	FAM65A	-1483	379	1.3	4.3	pN+	0.84	0
63	NDST3	-1270	345	3.8	9.2	pN+	0.84	0
64	LNX1	-1767	219	0.2	2.2	pN+	0.84	0.01
65	RNF212	239	528	3.7	8.8	pN+	0.84	0
66	SNORA74	-1681	241	3.5	1.7	pN0	0.84	0.02
67	MAPK11	-2018	386	5	2.8	pN0	0.84	0
68	Y_RNA	358	136	0.5	3	pN+	0.84	0.03
69	TRIP6	-1802	269	2.2	5.8	pN+	0.85	0.01
70	SLC7A7	629	477	1.2	4	pN+	0.85	0.01
71	FBRS	0	274	0.8	3.2	pN+	0.85	0
72	LRRC15	-707	26	2.2	0.7	pN0	0.85	0.02
73	DRGX	587	365	0.5	2.8	pN+	0.85	0.03
74	C19orf59	-1618	261	1.7	4.8	pN+	0.85	0
75	MYL2	-1098	122	0.5	2.7	pN+	0.85	0
76	PRX	-402	170	3	1.3	pN0	0.86	0.01
77	U4	37	233	4.5	2.5	pN0	0.86	0.01
78	DNAJC1	-931	180	1	3.7	pN+	0.86	0.02
79	NAPSB	488	67	0	1.8	pN+	0.86	0
80	PSG5	-1783	131	0.5	2.7	pN+	0.86	0
81	VNN1	-612	215	1.5	4.5	pN+	0.86	0
82	GTF2H3	-1896	98	2	5.5	pN+	0.86	0
83	DDA1	-1311	219	1.8	5.2	pN+	0.86	0
84	C16orf63	-1870	37	1.3	0	pN0	0.87	0
85	TJP2	50	288	1.5	4.5	pN+	0.87	0
86	SPATS2	-747	223	0.5	2.5	pN+	0.87	0
87	HS3ST5	540	115	0.2	2	pN+	0.87	0
88	AC135457.3	-1667	468	2	5.5	pN+	0.87	0.01
89	U6	-1218	313	1.3	4.3	pN+	0.87	0.03
90	METTL1	-1833	99	0.5	2.5	pN+	0.87	0
91	DKK4	433	164	4.7	2.7	pN0	0.87	0.03
92	U6	-1337	169	0.5	2.5	pN+	0.87	0
93	IZUMO1	269	496	2.7	6.7	pN+	0.87	0.01
94	HADHA	-1793	234	1.3	4.2	pN+	0.87	0
95	FOXRED2	-1075	343	3.7	8.5	pN+	0.87	0
96	AC120053.2	-891	118	1.7	4.8	pN+	0.87	0.01
97	DIRC3	19	263	2.7	6.7	pN+	0.88	0
98	Y_RNA	135	30	0.3	2.3	pN+	0.88	0.02
99	C17orf87	-1723	272	2.5	6.3	pN+	0.88	0
100	PKNOX1	0	281	2.2	5.7	pN+	0.88	0
101	RNF11	-1696	258	0.8	3.2	pN+	0.88	0
102	FTSJD1	-1907	103	1.3	0	pN0	0.88	0
103	PI16	-1349	177	1.8	5	pN+	0.88	0
104	SULT1A2	145	323	3.5	1.8	pN0	0.88	0
105	C20orf191	-2109	284	2	5.3	pN+	0.88	0.01
106	BPIL3	-1232	387	4.3	2.5	pN0	0.88	0.03
107	GTF3C2	-1891	232	1.8	5	pN+	0.89	0.01
108	SLC9A7	0	16	0.5	2.5	pN+	0.89	0
109	SCFD1	-1508	236	3	7.2	pN+	0.89	0.01
110	C1QB	-729	380	2.3	5.8	pN+	0.89	0
111	SRP_euk_arch	-1368	134	0.7	2.8	pN+	0.89	0.02
112	ZBTB34	-806	97	1.7	0.3	pN0	0.89	0.03
113	U6	-1268	88	0.5	2.5	pN+	0.89	0.01
114	C1orf198	-1498	76	1.5	4.3	pN+	0.89	0.02
115	SAMM50	0	358	2.5	6.2	pN+	0.89	0
116	MED31	-375	255	2	0.7	pN0	0.89	0.02
117	GLS	-1270	315	1.8	5	pN+	0.89	0.03
118	MYL2	-534	300	2.7	6.5	pN+	0.89	0.01
119	LY6H	-1414	85	2	0.7	pN0	0.9	0.02
120	RNH1	-1377	189	2.7	6.5	pN+	0.9	0.01
121	C6orf222	221	30	1.8	0.5	pN0	0.9	0.03
122	OR5AR1	0	1	1.8	0.5	pN0	0.9	0.05
123	SNORD115	-631	14	0.3	2.2	pN+	0.9	0.01
124	U6	-1756	311	1.7	4.5	pN+	0.9	0.01
125	NOL10	-755	401	2	5.2	pN+	0.9	0
126	U6atac	-103	413	1.8	4.8	pN+	0.9	0.01
127	snoU13	-344	214	1	3.3	pN+	0.9	0.01
128	VPRBP	0	123	1.7	4.5	pN+	0.9	0.05
129	TBX2	-1493	249	1.8	4.8	pN+	0.9	0
130	TBC1D12	-1236	314	3.3	7.7	pN+	0.9	0
131	SNORA32	-930	171	1	3.3	pN+	0.9	0.02

132	SETD4	0	234	1.3	4	pN+	0.9	0.03
133	SYNJ1	-1360	277	3.3	7.7	pN+	0.9	0
134	LSM8	-1377	279	2.3	5.7	pN+	0.9	0
135	ACIN1	-1207	409	3.2	7.3	pN+	0.9	0
136	INSM2	0	504	1.3	4	pN+	0.9	0.03
137	TADA1L	-1946	139	1	3.3	pN+	0.91	0.02
138	NCK1	0	32	0.8	2.8	pN+	0.91	0
139	IFT74	0	146	0.7	2.7	pN+	0.91	0
140	AC067852.1	-1723	141	1.2	3.5	pN+	0.91	0
141	FAM125A	-1983	260	1.7	4.5	pN+	0.91	0
142	IMPA1	-1295	258	4.2	9.2	pN+	0.91	0
143	OR7A10	-451	94	0.3	2.2	pN+	0.91	0.02
144	GABARAPL2	-757	225	2.5	1.2	pN0	0.91	0.01
145	ZNF490	-636	615	2.8	6.7	pN+	0.91	0.01
146	PROM1	-37	58	0.7	2.7	pN+	0.91	0.01
147	NEUROD6	-86	112	0.5	2.3	pN+	0.91	0
148	KLHDC8B	-2109	309	2.2	5.3	pN+	0.91	0
149	RP3-470B24.1	0	534	5.5	11.8	pN+	0.91	0
150	WDR33	-396	279	0.5	2.3	pN+	0.91	0
151	ZNF785	-1061	426	3.7	8.2	pN+	0.91	0.01
152	COBLL1	-1247	191	1.2	3.5	pN+	0.91	0.01
153	ALDOC	22	439	0.5	2.5	pN+	0.91	0.05
154	PARP12	301	397	1.3	3.8	pN+	0.91	0.01
155	OR4M1	522	228	1.2	3.5	pN+	0.91	0.01
156	L1TD1	-109	227	3.2	7.2	pN+	0.91	0
157	SRP_euk_arch	417	192	0.8	2.8	pN+	0.91	0
158	RP11-413E6.2	482	85	0.7	2.7	pN+	0.91	0.02
159	HUNK	-1704	375	3	6.8	pN+	0.92	0.01
160	ADAM8	-1894	57	0	1.7	pN+	0.92	0.01
161	TIMP4	-499	375	2.2	5.3	pN+	0.92	0
162	PIN1	-1045	559	2.7	6.2	pN+	0.92	0.01
163	CRIP3	367	1	0	1.5	pN+	0.92	0
164	AE000659.4	-1519	186	1.3	3.8	pN+	0.92	0.02
165	LMX1A	681	417	0.5	2.3	pN+	0.92	0.02
166	EIF2AK1	-539	336	2.7	6.2	pN+	0.92	0
167	CLEC14A	6	401	2.8	6.5	pN+	0.92	0
168	WIF1	-1274	1	0	1.7	pN+	0.92	0.04
169	FAM171A1	-1954	1	1.3	0.2	pN0	0.92	0
170	Y_RNA	-1717	291	1.8	4.7	pN+	0.92	0.02
171	LILRB1	0	115	1.8	0.7	pN0	0.93	0.01
172	GLI1	-1573	120	1.8	0.7	pN0	0.93	0.01
173	AL512662.7	244	41	1.8	0.7	pN0	0.93	0.01
174	OR5AR1	0	1	1.7	0.5	pN0	0.93	0.03
175	C2orf21	0	204	0.8	2.8	pN+	0.93	0
176	B4GALNT2	123	445	0.8	2.8	pN+	0.93	0
177	NLE1	-632	203	0.8	2.8	pN+	0.93	0.01
178	snoU13	-2125	382	2.2	5.2	pN+	0.93	0
179	ZNF24	-837	91	0.3	2	pN+	0.93	0.01
180	U5	524	599	0.7	2.3	pN+	0.93	0.01
181	MGMT	-1916	174	1.8	0.7	pN0	0.93	0.05
182	KATNAL2	-2019	151	0	1.5	pN+	0.93	0.01
183	Y_RNA	-1529	187	1.3	3.7	pN+	0.93	0
184	AGPAT3	0	286	2.8	6.3	pN+	0.93	0
185	ETF1	-1550	221	2	4.8	pN+	0.93	0.02
186	hsa-mir-320b-1	-706	1	1.2	0	pN0	0.93	0.02
187	B3GALNT2	-1540	127	2	4.8	pN+	0.93	0.01
188	ELAVL2	0	290	2.8	6.3	pN+	0.93	0.01
189	MBD1	-419	181	1.7	4.2	pN+	0.93	0.01
190	SLC45A4	-1753	100	3.7	7.8	pN+	0.93	0
191	TTLL4	0	373	5.8	12.2	pN+	0.93	0
192	KIAA1609	-1623	225	0.2	1.7	pN+	0.93	0
193	TACSTD2	561	641	1.2	3.3	pN+	0.93	0.01
194	EFCAB1	563	267	1.8	4.5	pN+	0.93	0.01
195	AMBN	-1442	273	2.5	5.7	pN+	0.93	0
196	SRP_euk_arch	240	74	1.2	0	pN0	0.94	0.02
197	METTL13	-972	39	0.2	1.7	pN+	0.94	0
198	RLBP1L2	69	361	3.5	7.5	pN+	0.94	0.02
199	BSDC1	-1670	160	0.5	2.2	pN+	0.94	0.01
200	C5orf46	-1265	228	0.5	2.2	pN+	0.94	0
201	HMGN1	-1629	1	1.2	0	pN0	0.94	0.03
202	GRHL2	85	533	0.5	2.2	pN+	0.94	0.01
203	TTC15	0	358	5.3	11	pN+	0.94	0
204	MT1F	-1401	143	0.2	1.7	pN+	0.94	0.01
205	ID4	0	57	1.2	0	pN0	0.94	0.03

206	C4orf50	-959	280	1.7	4.2	pN+	0.94	0.02
207	POTEH	78	142	0.5	2.2	pN+	0.94	0.03
208	B4GALNT4	545	468	3	6.5	pN+	0.94	0
209	ZAN	-296	299	1.5	3.8	pN+	0.94	0.01
210	C22orf9	-772	1	1.2	0	pN0	0.94	0.03
211	IGF2BP3	0	176	2	4.7	pN+	0.94	0
212	ATG4B	-1602	272	2.2	4.8	pN+	0.94	0.02
213	BCAN	-749	130	0.5	2.2	pN+	0.94	0.04
214	CRISPLD2	-501	283	1.3	3.5	pN+	0.94	0.02
215	C3orf54	-992	135	0.3	1.8	pN+	0.94	0
216	ZFP2	502	165	0.3	1.8	pN+	0.94	0
217	SRP_euk_arch	-1152	274	3	6.3	pN+	0.94	0.01
218	UBR7	-891	276	1.3	3.5	pN+	0.94	0
219	PPP4R2	-439	188	3	6.3	pN+	0.95	0.02
220	SLC10A6	-1106	68	0.3	1.8	pN+	0.95	0.01
221	AC092139.3	-482	418	1.8	4.3	pN+	0.95	0
222	GUCY2C	-1755	208	1.2	3.2	pN+	0.95	0.01
223	PPP4R4	-1345	80	2	1	pN0	0.95	0.02
224	CRIP3	360	1	0	1.3	pN+	0.95	0
225	C21orf32	633	302	1	2.8	pN+	0.95	0.01
226	DNA2	-1095	185	1.2	3.2	pN+	0.95	0.01
227	snoU13	-1534	70	1.2	3.2	pN+	0.95	0.01
228	TRIP6	-2067	260	3	6.3	pN+	0.95	0.01
229	U6	-59	136	1	2.8	pN+	0.95	0
230	CEL	-965	211	1.5	0.5	pN0	0.95	0.01
231	DEFB137	239	95	0.7	2.3	pN+	0.95	0.01
232	SH3RF3	0	293	3	6.3	pN+	0.95	0
233	GPD2	387	23	0.3	1.8	pN+	0.95	0.02
234	CRIP3	448	48	0	1.3	pN+	0.95	0
235	IGSF6	-1207	101	0.7	2.3	pN+	0.95	0.02
236	PPARD	-2016	146	1	2.8	pN+	0.95	0
237	C14orf167	-1893	19	0	1.3	pN+	0.95	0
238	HMX1	-362	310	1.8	0.8	pN0	0.95	0.02
239	SAR1B	-275	323	2.2	4.8	pN+	0.95	0
240	STK32B	-518	299	1.3	0.3	pN0	0.95	0.03
241	MCM2	0	260	2.2	4.8	pN+	0.95	0
242	RPP38	-601	156	1.3	0.3	pN0	0.95	0.03
243	RASL11B	-611	265	2.8	5.8	pN+	0.95	0.01
244	AL512624.1	-1134	255	5.8	11.7	pN+	0.95	0
245	Y_RNA	-790	227	1	2.7	pN+	0.95	0.02
246	TPM2	0	132	1	0	pN0	0.95	0
247	AC008537.3	0	84	1	0	pN0	0.95	0
248	NOC3L	-629	379	2	4.5	pN+	0.95	0.01
249	AC079354.2	0	415	3.3	6.8	pN+	0.95	0
250	PIF1	-1671	702	3	6.2	pN+	0.95	0.01
251	ZNF296	459	671	0.5	2	pN+	0.95	0.01
252	SFRS4	-714	269	0.8	2.5	pN+	0.95	0
253	THBS2	-1189	213	0.8	2.5	pN+	0.95	0
254	CASP12	-1748	176	1.3	3.3	pN+	0.95	0
255	DLGAP1	-481	439	4.2	8.3	pN+	0.95	0
256	SPANXN3	288	24	0	1.3	pN+	0.95	0.01
257	HK1	0	437	1.3	3.3	pN+	0.95	0.01
258	BBS2	-1332	96	0.5	2	pN+	0.95	0.01
259	snoU13	-2034	259	3.3	6.7	pN+	0.95	0.01
260	LRFN2	523	333	0.5	2	pN+	0.96	0.02
261	C1orf113	-66	419	1.2	3	pN+	0.96	0.01
262	GPR97	-1379	66	0.2	1.5	pN+	0.96	0
263	PDXK	-1433	252	0.5	2	pN+	0.96	0.02
264	PIAS4	-1474	275	3.8	7.7	pN+	0.96	0
265	RPS10L	-1511	253	0.2	1.5	pN+	0.96	0
266	SRP_euk_arch	-2258	683	1.8	4.2	pN+	0.96	0.01
267	SYPL2	425	157	0	1.3	pN+	0.96	0.02
268	TMEM98	-1560	16	0.5	2	pN+	0.96	0.05

Supplemental table 3.2. Statistical results and position information Infinium 450k for all WISP1 probes from the TCGA database.

Probe name	Chromosome	CpG location	CpG region	CpG Island location	Distance to WISP1 TSS	False Discovery Rate	Hypermethylated in
cg17218062	8	134218279	Open Sea	Not applicable	-6996	<0.00	pN+
cg25152058	8	134222322	CpG shore	Not applicable	-2953	<0.00	pN0
cg18802332	**8**	**134202353**	**CpG Island**	**134202271-134202560**	**-928**	**<0.00**	**pN0**
cg00122628	**8**	**134202359**	**CpG Island**	**134202271-134202560**	**-922**	**<0.00**	**pN0**
cg03670238	**8**	**134202370**	**CpG Island**	**134202271-134202560**	**-911**	**<0.00**	**pN0**
cg04421974	8	134224814	CpG Island	134224423-134224998	-461	<0.05	pN+
cg15463563	8	134224890	CpG Island	134224423-134224998	-385	<0.00	pN+
cg20257866	8	134203235	CpG Island	134203188-134203458	-46	<0.00	pN0
cg04683149	8	134203304	CpG Island	134203188-134203458	23	<0.00	pN+
cg26617637	8	134203339	CpG Island	134203188-134203458	58	<0.00	pN0
cg02903822	8	134203379	CpG Island	134203188-134203458	98	<0.05	pN0
cg02745822	8	134203435	CpG Island	134203188-134203458	154	<0.00	pN0
cg10191240	8	134230101	Open Sea	Not applicable	4826	<0.00	pN0
cg14929805	8	134232964	CpG Island	134232724-134233195	7689	<0.00	pN0

False Discovery Rate (Benjamini Heinberg) and direction of the differential methylation between the TCGA pN0 (n=61) and pN+ (n=87) OSCC for all WISP1 TSS associated Infinium 450k probes and all probe location info according to the GSE42409 database [242]. The probes that overlap with the MC identified by MethylCap-Seq are marked in bold (see Figure 3.1).